

Identification of a *CCDC114* variant in a Han-Chinese patient with situs inversus

XIANGYU CHEN^{1*}, SHENG DENG^{1,2*}, HONG XIA³, LAMEI YUAN¹,
HONGBO XU¹, SHIYU TANG¹ and HAO DENG^{1,4}

¹Center for Experimental Medicine, The Third Xiangya Hospital, Central South University, Changsha, Hunan 410013;

²Department of Pharmacy, Xiangya Hospital, Central South University, Changsha, Hunan 410008;

Departments of ³Emergency and ⁴Neurology, The Third Xiangya Hospital,
Central South University, Changsha, Hunan 410013, P.R. China

Received October 15, 2019; Accepted February 18, 2020

DOI: 10.3892/etm.2020.9059

Abstract. The function and position of the internal organs within the human body are based on left-right (LR) asymmetry. Human LR asymmetry disorders are characterized by abnormal LR asymmetric arrangement of the internal organs resulting from defective embryonic nodal cilia and nodal signaling pathway. The coiled-coil domain containing 114 gene (*CCDC114*) is related to the biogenesis of cilia and attachment of the outer dynein arms (ODAs) to the axoneme of cilia. Mutations in the *CCDC114* gene are reported to cause a subtype of primary ciliary dyskinesia (PCD) named ciliary dyskinesia, primary, 20 (CILD20). Patients with *CCDC114* mutations present with a type of ciliopathy with high clinical heterogeneity. In the present study, a Han-Chinese patient with situs inversus was recruited. Exome sequencing was performed on this patient combined with variant validation by Sanger sequencing. A homozygous variant c.584T>C (p.L195P) in the *CCDC114* gene was identified as the likely genetic cause for situs inversus in this patient. The findings of our study extend the mutational spectrum of the *CCDC114* gene, and contribute to clarifying the pathogenesis of human ciliopathies and benefit genetic counseling.

Introduction

Internal organs of the human and other vertebrates exhibit a highly conserved left-right (LR) asymmetry arrangement which is the base for their function and position (1,2). The

normal organ asymmetry arrangement across the LR axis is termed as situs solitus (3,4). LR asymmetry disorders occur as a result of genetic defects in the motile cilia of the embryonic node and nodal signaling pathway (5,6). The cilia-mediated fluid flow plays a critical role in the establishment of LR asymmetry arrangement during early embryonic development (7). Human LR asymmetry disorders with a minimum incidence of 1 per 8,000 newborns, can be divided into two categories, including situs inversus (complete mirror-image reversal of the internal organs) and situs ambiguus (abnormal arrangement of the internal organs, also named heterotaxy) (1,4). Situs inversus is also named situs inversus with dextrocardia for mirror-image anatomical topography of the heart (8,9). Situs inversus occurs in approximately half of patients with primary ciliary dyskinesia (PCD), while situs ambiguus occurs in no less than 12% of PCD patients (8). PCD is a ciliary disorder characterized by LR asymmetry disorder, neonatal respiratory distress, male infertility, and chronic oto-sino-pulmonary disease (10,11). Other rare symptoms including female infertility, hydrocephalus and retinitis pigmentosa have also been observed (6,12). Most of PCD cases are inherited in an autosomal recessive inheritance pattern, and a few have autosomal dominant or X-linked inheritance (8,13). Mutations in the genes associated with the establishment and function of nodal cilia are one of the genetic causes of human LR asymmetry disorders (4,12). No less than 69 genes have been reported to be associated with human LR asymmetry disorders (5,13-22). Mutations in the coiled-coil domain containing 114 gene (*CCDC114*), encoding a ciliary protein necessary for the attachment of the outer dynein arms (ODAs) to the axoneme of cilia, are reported to cause a subtype of PCD named ciliary dyskinesia, primary, 20 (CILD20) (23).

In the present study, a combination of exome sequencing and Sanger sequencing was used to identify the disease-causing gene and variant for a Han-Chinese patient with situs inversus. As a result, a homozygous variant, c.584T>C (p.L195P), in the *CCDC114* gene, was identified in the patient with situs inversus.

Correspondence to: Professor Hao Deng, Center for Experimental Medicine, The Third Xiangya Hospital, Central South University, 138 Tongzipo Road, Changsha, Hunan 410013, P.R. China
E-mail: hdeng008@yahoo.com

*Contributed equally

Key words: coiled-coil domain containing 114, situs inversus, primary ciliary dyskinesia, exome sequencing, variant

Patient and methods

Participators and clinical data. A 62-year-old female patient diagnosed with mirror-image dextrocardia using

a 12-lead electrocardiogram, in addition to a 59-year-old unrelated healthy female without any off-target condition, were recruited from the Third Xiangya Hospital, Central South University (Changsha, China) in December, 2018. The medical record of the patient was scrutinized and routine physical and radiological examinations were performed on the patient. The medical history of her deceased parents was also scanned. Written informed consent was obtained from the patient and the healthy individual before venous blood was sampled. The entire study was approved by the Institutional Review Board of the Third Xiangya Hospital, Central South University (Changsha, China) and carried out in accordance with the Declaration of Helsinki as revised in 2013.

Exome capture. After being extracted from peripheral blood samples by using the standard method described in a previous study (24), the genomic DNA (gDNA) of the proband was quantified by Qubit dsDNA HS Assay Kit (Invitrogen; Thermo Fisher Scientific, Inc.), and its integrity and purity were qualified on 1% agarose gel. An exome library was constructed with 1 μ g gDNA. It was sheared into fragments using Covaris E220 (Covaris, Inc.) and those with sizes of between 150 and 250 bp were selected using Agencourt AMPure XP Kit (Beckman Coulter Inc.). After being subjected to end-repairing, A-tailing reactions and adaptor ligation, the ligated fragments were enriched via amplification, purification and hybridization, using Agilent SureSelect Human All Exon V6 (cat. no. 5190-8872; Agilent Technologies, Inc.) and Agencourt AMPure XP Kit (Beckman Coulter Inc.). Following circularization with T4 DNA Ligase (cat. no. L6030-LC-L; Enzymatics Inc.; Qiagen GmbH), captured enrichment was processed by rolling circle amplification to form DNA nanoballs, which were then loaded onto a sequencing chip with a concentration of 40 ng/ μ l to be sequenced using MGISEQ-2000RS High-throughput Sequencing Set (FCL PE100; cat. no. 1000012554; BGI group). Paired-end sequencing with read lengths of 100 bp was performed on BGISEQ-500 sequencing platforms (BGI group) using combinatorial probe-anchor synthesis. All of the aforementioned experimental operations were performed in accordance to the manufacturers' protocols.

Read mapping and variant analysis. The raw data was processed to clean data which was mapped to the human reference genome (GRCh37/hg19) using Burrows Wheeler Aligner (BWA; version 0.7.15) (25). Remove of duplicated sequence by Picard (version 2.5.0, <https://broadinstitute.github.io/picard/>) and realignment by Genome Analysis Toolkit (GATK v3.3.0, <https://gatk.broadinstitute.org/hc/en-us>) were performed for accurate variant calling (26). Insertions-deletions (indels) and single nucleotide polymorphisms (SNPs) were called using HaplotypeCaller of GATK. Variants were annotated by SnpEff software (http://snpeff.sourceforge.net/SnpEff_manual.html) (27), and filtered against public databases including the Single Nucleotide Polymorphism database (dbSNP build 141) (28), 1000 Genomes Project (29) and the NHLBI exome sequencing project (ESP) 6500 (30), and an in-house



Figure 1. Chest X-ray of the patient with situs inversus.

exome database of BGI-Shenzhen (BGI group). The causative variants were confirmed by Sanger sequencing with ABI 3500 sequencer (Applied Biosystems; Thermo Fisher Scientific, Inc.) (31). The following are the sequences of primers for potential causative variant in the patient: Forward, 5'-CAGTCCAGCCTCCAGTCATC-3' and reverse, 5'-TTTTACGC TTCTCCAGGAC-3'.

Bioinformatic analyses. The possible impacts of variants on protein structure or function were predicted by several bioinformatic prediction software programs including MutationTaster (32), Protein Analysis Through Evolutionary Relationships (PANTHER) (33) and Protein Variation Effect Analyzer (PROVEAN) (34,35). A further conservative assessment of the amino acid at the variant position among different species was performed with the National Center for Biotechnology Information-Basic Local Alignment Search Tool (<https://blast.ncbi.nlm.nih.gov/Blast.cgi>) (36,37). Protean program of DNASTar's Lasergene v7.1.0 (DNASTAR, Inc.) was used to predict whether the candidate variant affected the protein secondary structure (38).

Quantitative PCR (qPCR). qPCR was performed to check the possible deletion involving candidate variant position using a LightCycler[®] 480 Instrument II (Roche) with qPCR SYBR Green Master Mix (Vazyme Biotech Co., Ltd.). The primers for the possible deletion were as follows: 5'-CAGTCCAGCCTCCAGTCATC-3' and 5'-ACCTGCGCCTCCATCTCG-3'. The gDNA sample of the healthy individual was used as the reference control. The glyceraldehyde-3-phosphate dehydrogenase gene (*GAPDH*) served as the reference gene and the primers were: 5'-CAC TCCTCCACCTTTGACGC-3' and 5'-CCACCACCCTGT TGCTGTAG-3'. Each reaction was conducted in triplicate. A repeated experiment was performed with the reference ATP binding cassette subfamily A member 4 gene (*ABCA4*) to ensure repeatability, and the primers were as previously

Table I. Clinical characteristics and genotypes of patients with *CCDC114* variants.

Study (ref.)	Patient	Sex	Age (years)	Situs	Neo RDS	Bxsis	Sinusitis	Otitis media	Other symptoms	Variant	Zygoty	
Onoufriadis <i>et al</i> , 2013 (23)	Family 1	II:3	M	NA	SS	-	+	+	+	-	c.742G>A	Homozygote
		II:4	M	NA	DEX	NA	+	+	-	-		
	II:7	F	NA	NA	NA	NA	NA	NA	NA			
	III:1	M	NA	SS	+	NA	+	+	CHD			
	III:2	M	NA	SI	-	NA	+	+	-			
	III:3	M	NA	SI	-	NA	-	+	-			
	III:5	F	NA	SS	-	+	-	+	-			
	III:8	M	NA	SS	-	NA	-	+	-			
	Family 2	II:2	F	NA	SS	-	+	+	+	-		
	Family 3	I:1	F	NA	SS	NA	+	+	+	-		
	Family 4	II:1	M	NA	SS	-	NA	-	+	-		
		II:2	F	NA	Abdominal SI	-	NA	-	+	-		
	Family 5	II:1	F	NA	SS	-	NA	NA	+	-		
Family 6	II:1	M	NA	SS	-	NA	+	+	-			
Family 7	II:1	M	NA	SI with medial heart position	-	NA	-	+	CHD			
Family 8	II:1	F	NA	SI	+	NA	-	-	-			
Family 9	II:1	F	NA	SI	-	+	+	+	CHD	c.486+1G>A	Homozygote	
Knowles <i>et al</i> , 2013 (55)	Family 10	III:1	F	39	SS	+	+	+	+	-		c.742G>A
		III:3	F	33	SS	+	+	+	+	-		
Family 11	I:3	F	59	SS	+	+	+	+	-	c.742G>A;	Compound heterozygote	
												c.487-2A>G
Family 12	IV:3	M	3	SS	+	-	-	+	-	c.1391+5G>A	Compound heterozygote	
												Family 13
II:2	F	34	SS	-	+	+	+	-	c.939delT			
										Li <i>et al</i> , 2019 (52)	Family 14	III:1
Present study	Family 15	II:1	F	62	SI	-	-	-	-			

CCDC114, the coiled-coil domain containing 114 gene; M, male; F, female; SS, situs solitus; SI, situs inversus; DEX, dextrocardia; Neo RDS, neonatal respiratory distress; Bxsis, bronchiectasis; CHD, congenital heart disease; +, present; -, absent; NA, not available.

published (39): 5'-ACCCAAGTATGGCCCCGTCCA-3' and 5'-TCCCATCCATCTGTTGCAGG-3'. The relative copy numbers of the candidate gene were evaluated using the comparative quantification cycle ($2^{-\Delta\Delta Cq}$) method (40). Statistical analysis was performed using the Microsoft Excel 2016 software (Microsoft, Inc.) and GraphPad Prism v8.0.2 (GraphPad Software, Inc.) using a two-tailed unpaired Student's t-test.

Results

Clinical findings. Chest radiograph revealed the mirror-image reversal of the heart and gastric bubble in the patient (Fig. 1), and no other classical PCD symptoms were observed, which agreed with the diagnosis of situs inversus (Table I). The medical history of her deceased parents suggested a negative family history in her family (Fig. 2A).

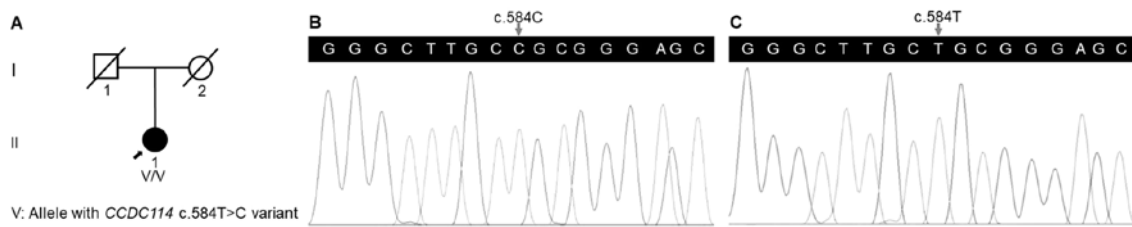


Figure 2. (A) Pedigree of a Han-Chinese patient with situs inversus. Square represents male; circles represent females; slashed symbols represent deceased individuals; darkened symbol symbolizes patient with situs inversus; arrow presents the proband. (B) Sequence of the homozygous c.584T>C (p.L195P) variant in the proband. (C) Sequence of the wild-type *CCDC114* gene in the healthy individual. *CCDC114*, the coiled-coil domain containing 114 gene.

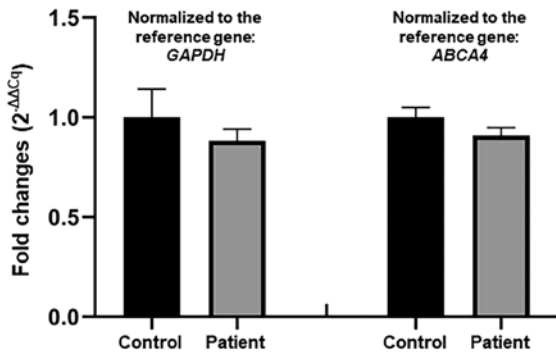


Figure 3. Relative quantification of the *CCDC114* gene in the patient and a healthy individual by genomic quantitative PCR. *CCDC114*, the coiled-coil domain containing 114 gene.

Variant screening. A total of 142.67 million effective reads were generated from exome sequencing of the patient. Among them, 99.94% were successful in mapping to the human reference genome. The target sequence covered 99.48% of bases at $\geq x10$ with an average sequencing depth of $x177.41$. A total of 97,358 SNPs and 16,875 indels were detected in the patient. A variant filtering strategy as described in recent studies was utilized for confirming the potential causative variant for the patient (39,41): i) Variants documented in dbSNP141, 1000 Genomes Project and NHLBI ESP6500 with a minor allele frequency $>0.1\%$ were excluded; ii) among the remaining, variants absent in 1,943 additional Chinese controls without LR asymmetry disorder from an in-house exome database of BGI-Shenzhen were preferred for the next analysis; and iii) variants predicted to be deleterious by *in silico* tools were reserved. Using the aforementioned criteria, a variant in the *CCDC114* gene (reference sequence: NM_144577.4), c.584T>C (p.L195P), was selected as the most possible disease-causing variant for the patient. Sanger sequencing validated the variant in the patient (Fig. 2B) and its absence in the healthy individual (Fig. 2C). The qPCR analysis confirmed no deletion of the *CCDC114* gene involving the variant position in the patient (Fig. 3).

Bioinformatic analyses. The *CCDC114* variant c.584T>C (p.L195P), was predicted to be disease-causing by MutationTaster with a probability score of ~ 1 , possibly damaging by PANTHER with the position in the protein evolutionarily conserved for >200 million years (preservation time, 220 million years), and deleterious by PROVEAN with a score of -5.99 . These indicated that the protein structure and function were possibly affected by

this variant, which is consistent with the high conservation of the p.L195 residue among nine vertebrates (Fig. 4A). This variant was predicted to change the secondary structure of *CCDC114* by Protean based on the Chou-Fasman method (Fig. 4B). An α -helix (residues 181-230) was predicted to be broken into two α -helices (residues 181-193 and residues 196-230) by the c.584T>C variant. Based on the above evidence, the variant c.584T>C in the *CCDC114* gene appears to be accountable for the situs inversus in this patient.

Discussion

The normal human body displays an obvious LR asymmetry in the placement and structure of the internal organs (42). The perturbation of human LR asymmetry gives rise to disorders including situs inversus and situs ambiguus (43). The generation of LR asymmetry depends on LR side-specific cascades of gene expression during early embryogenesis. The process can be divided into four distinct phases: i) the bilateral symmetry breaking of the early embryo; ii) asymmetric signals transduced from the node to lateral plate mesoderm (LPM); iii) cascades of LR asymmetric gene expression in the left LPM; and iv) LR asymmetric morphogenesis (5,44).

Abnormal embryonic nodal cilia and perturbation in the nodal signaling pathway are two causes for human LR asymmetry disorders (5). A group of human LR asymmetry disorders resulting from dysmotility or absence of embryonic nodal cilia can be regarded as a type of ciliopathy (45). Cilia and flagella are hair-like organelles in eukaryotic cells. A cilium is composed of a basal body, transition zone, axoneme, ciliary membrane, and the ciliary tip. The axoneme is the main part of the cilium, and the basal body inside the cell plays a role in anchoring the cilium (45-47). The axoneme is assembled by nine peripheral microtubule doublets, surrounding a central pair of microtubules (9+2 pattern) or absence of the central microtubules (9+0 pattern) (48). Each peripheral doublet microtubule possesses an outer dynein arm (ODA) and an inner dynein arm (IDA) (6). The nodal motile cilium with a 9+0 axonemal configuration without central pair existing in the early embryo, has dynein arms and nine peripheral doublets (11). Gene-targeted therapy during early embryogenesis that aimed to normalize the nodal signaling pathway or the function of embryonic nodal cilia may be helpful for rescuing the perturbation of human LR asymmetry.

The *CCDC114* gene is located at chromosome 19q13.33 and is composed of 14 exons. The ciliary protein, *CCDC114*, as a

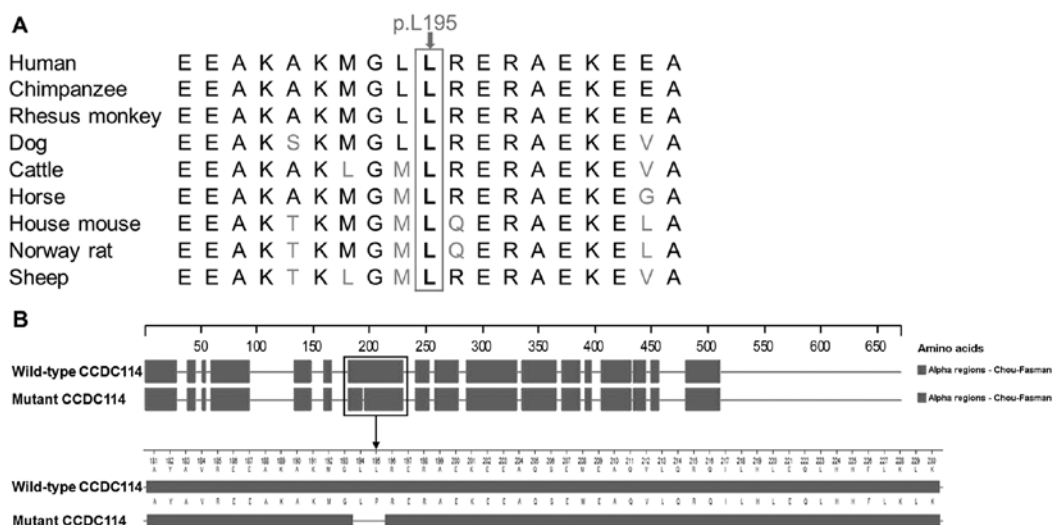


Figure 4. (A) Conservation analysis of the p.L195 residue in CCDC114 among nine different vertebrates. (B) The α -helix conformations of wild-type and mutant CCDC114 predicted by Protean. An α -helix (residues 181-230) was disrupted at residues 194-195 by the variant. CCDC114, coiled-coil domain containing 114.

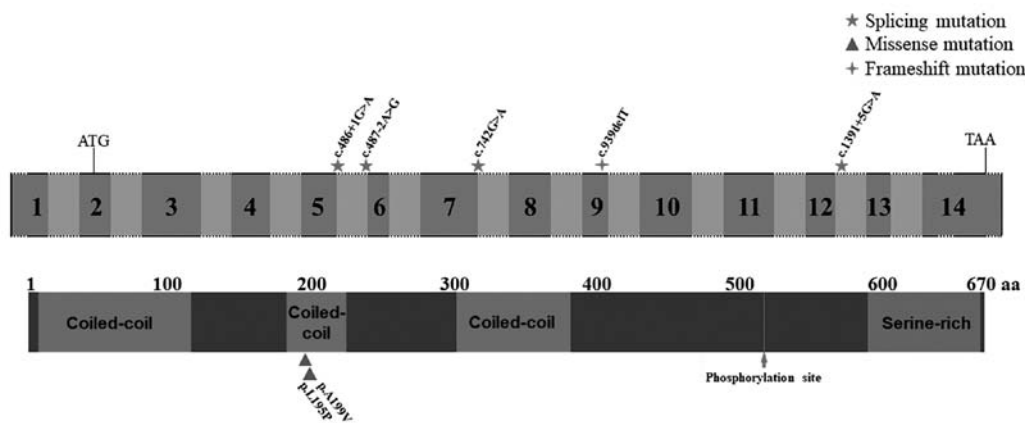


Figure 5. Schematic representation of the *CCDC114* gene and protein. Numbered boxes indicate exons, and unnumbered boxes indicate introns or intergenic regions. Regions indicated by dashed lines represent out-of-proportion exons or introns. All mutations were described following the *CCDC114* isoform (NM_144577.4, NP_653178.3). Three coiled-coil domains (residues 9-155, 183-224, and 302-381), a phosphorylation site (p.S517) and a serine-rich region (residues 590-668) were shown in the protein. *CCDC114*, the coiled-coil domain containing 114 gene. aa, amino acids.

component of ODA docking complex along with CCDC151, armadillo repeat containing protein 4, and tetratricopeptide repeat domain 25, may interact with meiosis specific nuclear structural 1 and dynein axonemal heavy chain 9 to participate in binding ODAs to outer doublet microtubules (17,20,21,23,49). The dynein arms containing ATPase provide a driving force (four-fifths from ODAs) for the sliding of peripheral doublet microtubules which generates ciliary beating (49,50). The genetic deficiency in *CCDC114* cause ODA defects, leading to immotile cilia. Impaired motile 9+2 cilia and flagella are responsible for PCD symptoms including neonatal respiratory distress, chronic oto-sino-pulmonary disease, infertility, and hydrocephalus, while human LR asymmetry disorders result from defective embryonic nodal motile (9+0) cilia (6,10). The nodal cilia clockwise rotary generates a leftward flow of extraembryonic fluid, which results in the breakage of the bilateral symmetry (51). Mutations in the *CCDC114* gene are known to cause CILD20 (OMIM 615067). Deficiency in *CCDC114* not only impairs ODA of motile cilia but also impacts the biogenesis of primary cilia (23,52).

Various cases with mutations in ciliary protein and displaying partial PCD symptoms but imperfect for the standard clinical diagnostic criteria for PCD have also been reported (14,17). In the present study, a patient presented with situs inversus but no other PCD symptoms were reported, and a missense variant c.584T>C (p.L195P) located in the coiled-coil domain of the *CCDC114* protein was identified in her. The qPCR analysis confirmed no deletion of the *CCDC114* gene involving the variant position, validating the homozygosity of the c.584T>C variant. Although consanguineous marriage was denied in this family, the parents resided within the same village which may imply a possibility of founder effect (53). *In silico* tools including MutationTaster, PANTHER and PROVEAN predicted that the c.584T>C variant had deleterious effects on protein structure and function. This variant was absent in dbSNP141, 1000 Genomes Project, NHLBI ESP6500 and an in-house exome database of BGI-Shenzhen. It may change the secondary structure of *CCDC114* by breaking an α -helix (residues 181-230) at residues 194-195 based on Protean prediction. Further functional

studies, as well as co-segregation analyses in more families with situs inversus, are necessary for validating accurate clinical classification of this variant. Defective motile cilia in different tissues and organs underlie different PCD symptoms (54). The patient carrying homozygous *CCDC114* variant c.584T>C presented with situs inversus, suggesting that this missense variant mainly affects embryonic nodal cilia. Published articles accessed in the PubMed database reported 6 *CCDC114* mutations associated with PCD. Biallelic splice-site mutations in the *CCDC114* gene including homozygous mutations (c.742G>A and c.486+1G>A) and compound heterozygous mutations (c.742G>A and c.487-2A>G, c.742G>A and c.1391+5G>A, and c.742G>A and c.939delT) were reported to cause classical PCD phenotype, while a homozygous c.596C>T (p.A199V) mutation was reported to cause PCD symptoms accompanied with other additional symptoms linked with defective primary cilia (Table I; Fig. 5) (23,52,55). No obvious phenotype-genotype correlation in *CCDC114* is observed. The phenotypic variation of *CCDC114*-associated ciliopathies suggested that one or more types of cilia may be involved by a single *CCDC114* mutation (52), which may be a random chance confounded by other genetic, epigenetic and environmental factors.

In summary, using exome sequencing and a significant filtration strategy, it was demonstrated that a *CCDC114* variant, c.584T>C (p.L195P), may be responsible for situs inversus in a Han-Chinese patient. To the best of our knowledge, the homozygous c.584T>C variant in the *CCDC114* gene is first reported as the disease-causing variant for situs inversus in the present study. Findings from the present study broaden the mutational spectrum of the *CCDC114* gene and assist the genetic counseling of human LR asymmetry disorders. In the future, more confirmation and functional studies of *CCDC114* mutations, and the establishment of deficient animal models with *CCDC114*-associated ciliopathies will facilitate an in-depth comprehension of molecular and cellular mechanisms of human ciliopathies.

Acknowledgements

Not applicable.

Funding

This study was supported by the National Natural Science Foundation of China (grant nos. 81670216, 81800219 and 81873686), the Natural Science Foundation of Hunan Province (grant no. 2018JJ2660), the Science and Technology Program of Hunan Province (grant no. 2017SK50131), the Scientific Research Project of Health and Family Planning Commission of Hunan Province, China (grant nos. B20180760 and B20180834), the Lotus Scholars Program of Hunan Province (to HD), the Hunan Provincial Innovation Foundation For Postgraduate (grant no. CX20190252) and the Undergraduate Innovative Training Plan Program of Central South University, China (grant no. XCX20190629).

Availability of data and materials

The datasets used and/or analyzed during the current study are available from the corresponding author on reasonable request.

Authors' contributions

XC, SD and HD conceived and designed this study. HX, ST and HD collected the patient samples and clinical data. XC, SD and HX performed the experiments; XC, LY and HD analyzed the data. XC, SD and HD wrote the manuscript. All authors read and approved the manuscript and agreed to be accountable for all aspects of the research in ensuring that the accuracy or integrity of any part of the work was appropriately investigated and resolved.

Ethics approval and consent to participate

The study was conducted in compliance with the Declaration of Helsinki Principles and with the consent of the Institutional Review Board of the Third Xiangya Hospital of Central South University in Changsha, Hunan, China (approval no. 2018-S400). Written informed consent was obtained from the participants prior to being included in the study.

Patient consent for publication

Not applicable.

Competing interests

The authors declare that they have no competing interests.

References

- Levin M: The embryonic origins of left-right asymmetry. *Crit Rev Oral Biol Med* 15: 197-206, 2004.
- Nakamura T and Hamada H: Left-right patterning: Conserved and divergent mechanisms. *Development* 139: 3257-3262, 2012.
- Blum M and Ott T: Animal left-right asymmetry. *Curr Biol* 28: R301-R304, 2018.
- Shapiro A, Davis S, Manion M and Briones K: Primary ciliary dyskinesia (PCD). *Am J Respir Crit Care Med* 198: P3-P4, 2018.
- Deng H, Xia H and Deng S: Genetic basis of human left-right asymmetry disorders. *Expert Rev Mol Med* 16: e19, 2015.
- Lee L: Mechanisms of mammalian ciliary motility: Insights from primary ciliary dyskinesia genetics. *Gene* 473: 57-66, 2011.
- Narasimhan V, Hjeij R, Vij S, Loges NT, Wallmeier J, Koerner-Rettberg C, Werner C, Thamilselvam SK, Boey A, Choksi SP, *et al*: Mutations in *CCDC11*, which encodes a coiled-coil containing ciliary protein, causes situs inversus due to dysmotility of monocilia in the left-right organizer. *Hum Mutat* 36: 307-318, 2015.
- Shapiro AJ, Zariwala MA, Ferkol T, Davis SD, Sagel SD, Dell SD, Rosenfeld M, Olivier KN, Milla C, Daniel SJ, *et al*: Diagnosis, monitoring, and treatment of primary ciliary dyskinesia: PCD foundation consensus recommendations based on state of the art review. *Pediatr Pulmonol* 51: 115-132, 2016.
- Zanatta A, Zampieri F, Bonati MR, Frescura C, Scattolin G, Stramare R and Thiene G: Situs inversus with dextrocardia in a mummy case. *Cardiovasc Pathol* 23: 61-64, 2014.
- Knowles MR, Zariwala M and Leigh M: Primary ciliary dyskinesia. *Clin Chest Med* 37: 449-461, 2016.
- Knowles MR, Daniels LA, Davis SD, Zariwala MA and Leigh MW: Primary ciliary dyskinesia. Recent advances in diagnostics, genetics, and characterization of clinical disease. *Am J Respir Crit Care Med* 188: 913-922, 2013.
- Boon M, Jorissen M, Proesmans M and De Boeck K: Primary ciliary dyskinesia, an orphan disease. *Eur J Pediatr* 172: 151-162, 2013.
- Wallmeier J, Frank D, Shoemark A, Nöthe-Menchen T, Cindric S, Olbrich H, Loges NT, Aprea I, Dougherty GW, Pennekamp P, *et al*: De novo mutations in *FOXJ1* result in a motile ciliopathy with hydrocephalus and randomization of left/right body asymmetry. *Am J Hum Genet* 105: 1030-1039, 2019.

14. Bonnefoy S, Watson CM, Kernohan KD, Lemos M, Hutchinson S, Poulter JA, Crinnion LA, Berry I, Simmonds J, Vasudevan P, *et al*: Biallelic mutations in LRRC56, encoding a protein associated with intraflagellar transport, cause mucociliary clearance and laterality defects. *Am J Hum Genet* 103: 727-739, 2018.
15. Vetrini F, D'Alessandro LC, Akdemir ZC, Braxton A, Azamian MS, Eldomery MK, Miller K, Kois C, Sack V, Shur N, *et al*: Bi-allelic mutations in PKD1L1 are associated with laterality defects in humans. *Am J Hum Genet* 99: 886-893, 2016.
16. Fassad MR, Shoemark A, le Borgne P, Koll F, Patel M, Dixon M, Hayward J, Richardson C, Frost E, Jenkins L, *et al*: C11orf70 mutations disrupting the intraflagellar transport-dependent assembly of multiple axonemal dyneins cause primary ciliary dyskinesia. *Am J Hum Genet* 102: 956-972, 2018.
17. Ta-Shma A, Hjeij R, Perles Z, Dougherty GW, Abu Zahira I, Letteboer SJF, Antony D, Darwish A, Mans DA, Spittler S, *et al*: Homozygous loss-of-function mutations in MNS1 cause laterality defects and likely male infertility. *PLoS Genet* 14: e1007602, 2018.
18. Perles Z, Moon S, Ta-Shma A, Yaacov B, Francescato L, Edvardson S, Rein AJ, Elpeleg O and Katsanis N: A human laterality disorder caused by a homozygous deleterious mutation in MMP21. *J Med Genet* 52: 840-847, 2015.
19. Paff T, Loges NT, Aprea I, Wu K, Bakey Z, Haarman EG, Daniels JMA, Siermans EA, Bogunovic N, Dougherty GW, *et al*: Mutations in PIH1D3 cause X-linked primary ciliary dyskinesia with outer and inner dynein arm defects. *Am J Hum Genet* 100: 160-168, 2017.
20. Loges NT, Antony D, Mavor A, Deardorff MA, Güleç EY, Gezdirici A, Nöthe-Menchen T, Höben IM, Jelten L, Frank D, *et al*: Recessive DNAH9 loss-of-function mutations cause laterality defects and subtle respiratory ciliary-beating defects. *Am J Hum Genet* 103: 995-1008, 2018.
21. Wallmeier J, Shiratori H, Dougherty GW, Edelbusch C, Hjeij R, Loges NT, Menchen T, Olbrich H, Pennekamp P, Raidt J, *et al*: TTC25 deficiency results in defects of the outer dynein arm docking machinery and primary ciliary dyskinesia with left-right body asymmetry randomization. *Am J Hum Genet* 99: 460-469, 2016.
22. Imtiaz F, Allam R, Ramzan K and Al-Sayed M: Variation in DNAH1 may contribute to primary ciliary dyskinesia. *BMC Med Genet* 16: 14, 2015.
23. Onoufriadis A, Paff T, Antony D, Shoemark A, Micha D, Kuyt B, Schmidts M, Petridi S, Dankert-Roelse JE, Haarman EG, *et al*: Splice-site mutations in the axonemal outer dynein arm docking complex gene CCDC114 cause primary ciliary dyskinesia. *Am J Hum Genet* 92: 88-98, 2013.
24. Chen X, Deng S, Xu H, Hou D, Hu P, Yang Y, Wen J, Deng H and Yuan L: Novel and recurring NOTCH3 mutations in two Chinese patients with CADASIL. *Neurodegener Dis* 19: 35-42, 2019.
25. Li H: Aligning sequence reads, clone sequences and assembly contigs with BWA-MEM. arXiv:1303.3997v2 (q-bio.GN). Oxford University Press, 2013.
26. Van der Auwera GA, Carneiro MO, Hartl C, Poplin R, Del Angel G, Levy-Moonshine A, Jordan T, Shakir K, Roazen D, Thibault J, *et al*: From FastQ data to high confidence variant calls: The Genome Analysis Toolkit best practices pipeline. *Curr Protoc Bioinformatics* 43: 11.10.1-11.10.33, 2013.
27. Cingolani P, Platts A, Wang le L, Coon M, Nguyen T, Wang L, Land SJ, Lu X and Ruden DM: A program for annotating and predicting the effects of single nucleotide polymorphisms, SnpEff: SNPs in the genome of *Drosophila melanogaster* strain w1118; iso-2; iso-3. *Fly (Austin)* 6: 80-92, 2012.
28. Sherry ST, Ward MH, Kholodov M, Baker J, Phan L, Smigielski EM and Sirotkin K: dbSNP: The NCBI database of genetic variation. *Nucleic Acids Res* 29: 308-311, 2001.
29. 1000 Genomes Project Consortium; Auton A, Brooks LD, Durbin RM, Garrison EP, Kang HM, Korbel JO, Marchini JL, McCarthy S, McVean GA, *et al*: A global reference for human genetic variation. *Nature* 526: 68-74, 2015.
30. NHLBI Exome Sequencing Project (ESP): Exome Variant Server. <http://evs.gs.washington.edu/EVS/>. Accessed 31 January, 2018.
31. Chen X, Yuan L, Xu H, Hu P, Yang Y, Guo Y, Guo Z and Deng H: Novel GLI3 mutations in Chinese patients with non-syndromic post-axial polydactyly. *Curr Mol Med* 19: 228-235, 2019.
32. Schwarz JM, Cooper DN, Schuelke M and Seelow D: MutationTaster2: Mutation prediction for the deep-sequencing age. *Nat Methods* 11: 361-362, 2014.
33. Mi H, Muruganujan A, Ebert D, Huang X and Thomas PD: PANTHER version 14: More genomes, a new PANTHER GO-slim and improvements in enrichment analysis tools. *Nucleic Acids Res* 47: D419-D426, 2019.
34. Choi Y and Chan AP: PROVEAN web server: A tool to predict the functional effect of amino acid substitutions and indels. *Bioinformatics* 31: 2745-2747, 2015.
35. Xiao H, Yuan L, Xu H, Yang Z, Huang F, Song Z, Yang Y, Zeng C and Deng H: Novel and recurring disease-causing NF1 variants in two Chinese families with neurofibromatosis type 1. *J Mol Neurosci* 65: 557-563, 2018.
36. Sayers EW, Beck J, Brister JR, Bolton EE, Canese K, Comeau DC, Funk K, Ketter A, Kim S, Kimchi A, *et al*: Database resources of the National Center for Biotechnology Information. *Nucleic Acids Res* 48: D9-D16, 2020.
37. Chen Q, Yuan L, Deng X, Yang Z, Zhang S, Deng S, Lu H and Deng H: A missense variant p.Ala117Ser in the transthyretin gene of a Han Chinese family with familial amyloid polyneuropathy. *Mol Neurobiol* 55: 4911-4917, 2018.
38. Burland TG: DNASTAR's Lasergene sequence analysis software. *Methods Mol Biol* 132: 71-91, 2000.
39. Xiang Q, Cao Y, Xu H, Guo Y, Yang Z, Xu L, Yuan L and Deng H: Identification of novel pathogenic ABCA4 variants in a Han Chinese family with Stargardt disease. *Biosci Rep* 39: BSR20180872, 2019.
40. Livak KJ and Schmittgen TD: Analysis of relative gene expression data using real-time quantitative PCR and the 2(-Delta Delta C(T)) method. *Methods* 25: 402-408, 2001.
41. Xiao H, Guo Y, Yi J, Xia H, Xu H, Yuan L, Hu P, Yang Z, He Z, Lu H and Deng H: Identification of a novel keratin 9 missense mutation in a Chinese family with epidermolytic palmoplantar keratoderma. *Cell Physiol Biochem* 46: 1919-1929, 2018.
42. Norris DP: Cilia, calcium and the basis of left-right asymmetry. *BMC Biol* 10: 102, 2012.
43. Huang S, Xu W, Su B and Luo L: Distinct mechanisms determine organ left-right asymmetry patterning in an uncoupled way. *Bioessays* 36: 293-304, 2014.
44. Mercola M: Left-right asymmetry: Nodal points. *J Cell Sci* 116: 3251-3257, 2003.
45. Reiter JF and Leroux MR: Genes and molecular pathways underpinning ciliopathies. *Nat Rev Mol Cell Biol* 18: 533-547, 2017.
46. Ishikawa T: Axoneme structure from motile cilia. *Cold Spring Harb Perspect Biol* 9: a028076, 2017.
47. Fliedrauf M, Benzing T and Omran H: When cilia go bad: Cilia defects and ciliopathies. *Nat Rev Mol Cell Biol* 8: 880-893, 2007.
48. Mitchison HM and Valente EM: Motile and non-motile cilia in human pathology: From function to phenotypes. *J Pathol* 241: 294-309, 2017.
49. Hjeij R, Onoufriadis A, Watson CM, Slagle CE, Klena NT, Dougherty GW, Kurkowiak M, Loges NT, Diggle CP, Morante NF, *et al*: CCDC151 mutations cause primary ciliary dyskinesia by disruption of the outer dynein arm docking complex formation. *Am J Hum Genet* 95: 257-274, 2014.
50. Ibañez-Tallon I, Heintz N and Omran H: To beat or not to beat: Roles of cilia in development and disease. *Hum Mol Genet* 12: R27-R35, 2003.
51. Eley L, Yates LM and Goodship JA: Cilia and disease. *Curr Opin Genet Dev* 15: 308-314, 2005.
52. Li P, He Y, Cai G, Xiao F, Yang J, Li Q and Chen X: CCDC114 is mutated in patient with a complex phenotype combining primary ciliary dyskinesia, sensorineural deafness, and renal disease. *J Hum Genet* 64: 39-48, 2019.
53. Chen H, Huang X, Yuan L, Xia H, Xu H, Yang Y, Zheng W and Deng H: A homozygous parkin p.G284R mutation in a Chinese family with autosomal recessive juvenile parkinsonism. *Neurosci Lett* 624: 100-104, 2016.
54. Wu DH and Singaraja RR: Loss-of-function mutations in CCDC114 cause primary ciliary dyskinesia. *Clin Genet* 83: 526-527, 2013.
55. Knowles MR, Leigh MW, Ostrowski LE, Huang L, Carson JL, Hazucha MJ, Yin W, Berg JS, Davis SD, Dell SD, *et al*: Exome sequencing identifies mutations in CCDC114 as a cause of primary ciliary dyskinesia. *Am J Hum Genet* 92: 99-106, 2013.